LUND UNIVERSITY

ACOUSTIC ANALYSIS OF LOUDSPEAKER CAVITY INCLUDING VISCOTHERMAL EFFECTS

BOEL HÖKMARK

Structural Mechanics

Master´s Dissertation

Department of Construction Sciences
Structural Mechanics

ISRN LUTVDG/TVSM--06/5142--SE (1-29)
ISSN 0281-6679

ACOUSTIC ANALYSIS OF LOUDSPEAKER CAVITY INCLUDING VISCOTHERMAL EFFECTS

Master's Dissertation by
BOEL HÖKMARK

Supervisors:
Per-Anders Wernberg,PhD, Div. of Structural Mechanics,
Jonas Brunskog, PhD., Div. of Engineering Acoustics
and Per Hiselius, PhD., Sony Ericsson Mobile Com.

Printed by KFS I Lund AB, Lund, Sweden, January, 2007.

For information, address:
Division of Structural Mechanics, LTH, Lund University, Box 118, SE-221 00 Lund, Sweden.
Homepage: http://www.byggmek.lth.se

Abstract

The geometry of a loud speaker cavity often gets a complicated geometry with sharp corners and narrow ducts. For this kind of shape the internal energy losses caused by viscosity and thermal conduction play an important role in the acoustic behavior. Today there is no method that sufficiently predict these effects. In this report the analogy between the loudspeaker cavity, a simple mass and spring system and a Helmholtz's resonator is very important. It shows that the damping at the eigen-frequencies corresponds to the acoustic impedance of the system. That was the reason that the aim of this master thesis was to create a finite element model of a loudspeaker cavity and with this calculate the acoustic impedance including the internal energy losses. The model was created by using a reliable approach of two equations. The first one describes the acoustic pressure and the second one describes the thermal conduction. The two equations can be used separated except at the boundaries where they are connected by the boundary conditions. This finite element model yields results that are totally damped, meaning that the model is not working. A reason for that could be that the mesh is too coarse. Another reason could be that the energy dissipating parameter bulk viscosity is not correctly implemented. One thing that made it difficult to implement was the lack of relevant values, another the fact that it seems to have different definitions for different kinds of applications.

Contents

Chapter 1

Introduction

1.1 Background

A mobile phone consists of many different components that all require a certain amount of space. The acoustic quality of the loudspeaker for example, is highly dependent on the loudspeakers cavity. This cavity sometimes gets a complex geometry with small ducts and narrow spaces. For this kind of shape the viscosity and the heat conduction play an important role in the acoustic behavior, especially for the acoustic response close to the eigen-frequencies. The viscosity and the heat conduction of the air, damp the amplitude of the frequency response which will result in a bad sound quality. Today there is no sufficient way to predict the damping effects of a certain geometry of a loudspeaker cavity. Instead, a lot of time consuming tests have to be done in order to develop and verify the sound. It would be advantageous and more cost efficient if the frequency response could be predicted in an earlier stage of the production.

1.2 Purpose

The purpose of this master thesis is to evaluate the possibilities to numerical calculate the complex acoustic impedance of a loudspeaker cavity, considering the effects of viscosity and thermal conduction.

1.3 Method

The geometry of the cavity is generated in ABAQUS. In order to get the resonance frequency in the right range the theory of Helmholtz's resonator is used. The idea is then to use already existing acoustic and thermal elements in Calfem, and include the loss of energy by means of the Stokes-Navier equation and thermodynamic relationships. This method will be compared to the alternative approach that is used in ABAQUS.

Chapter 2

Theory

2.1 The wave equation

The linearized wave equation is given by Equation 2.1[4].

$$\nabla^2 p - \frac{1}{c^2}\frac{\partial^2 p}{\partial t^2} = 0 \tag{2.1}$$

Here p denotes the acoustic pressure and c denotes the speed of sound which for air is about 340 m/s for normal conditions. The pressure in Equation 2.1 is described as a function of time. In this work, the analysis of the acoustic responses will be made as a function of frequency. Therefor, the time derivaty has to be transformed to a frequency dependent variable using the time harmonic relationship shown in Equation 2.2, where $\omega = 2\pi f$ denotes the angle velocity.

$$\begin{aligned} \frac{\partial}{\partial t} &= -i\omega \\ \frac{\partial^2}{\partial t^2} &= \omega^2 \end{aligned} \tag{2.2}$$

The acoustic pressure tends to cover a very wide range of frequencies. It is therefor convenient to use the logarithmic variable L_p, shown in Equation 2.3.

$$L_p = 10log\frac{|p|^2}{p_{ref}^2} = 20log\frac{|p|}{p_{ref}}[dB] \tag{2.3}$$

The reference pressure p_{ref} is set to $2 \cdot 10^{-5}$, which is the lowest pressure a human can here.

2.2 The acoustic impedance

The acoustic impedance given by Equation 2.4, is the ratio between the pressure and the particle velocity of a sound wave.

$$Z = \frac{p}{v} \tag{2.4}$$

The impedance and its relevance for this work will be discussed in section 2.3.

2.3 A damped oscillator

To understand the impact of the fundamental quantities, a simple one degree of freedom-system can be studied. An example of this system, a so called damped oscillator, is illustrated in Figure 2.1.

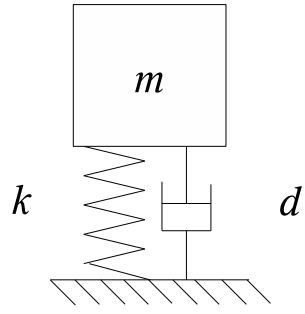

Figure 2.1: A damped oscillator. Here κ denotes the stiffness of the spring, d denotes the damping constant and m denotes the mass.

The second law of motion and the exciting effect of the force on the mass yield, with stiffness κ, damping constant d and the mass m, the differential equation 2.5[4]:

$$\frac{d^2x(t)}{dt^2} + 2\delta\frac{dx(t)}{dt} + \omega_0^2 x(t) = g(t) \tag{2.5}$$

where:

$$\omega_0 = \sqrt{\frac{k}{m}}, \quad \delta = \frac{d}{2m}, \quad g(t) = \frac{F(t)}{m} \tag{2.6}$$

The approaches $g(t) = \hat{g}e^{i\omega t}$ and $x_p(t) = x_p e^{i\omega t}$ yield for Equation 2.5 following particular solution[4]:

$$x_p = \frac{\hat{g}}{(\omega_0^2 - \omega^2) + i2\delta\omega} \tag{2.7}$$

From Equation 2.5 and 2.7, one can see that for frequencies below the eigenfrequency ($\omega < \omega_o$), the stiffness will determine the displacement, while the mass is decisive for high frequencies. Finally, for the frequencies corresponding to the eigenfrequencies ($\omega = \omega_o$), the particular solution is ending up in Equation 2.8 using the expressions for δ and $g(t)$ above.

$$x_p = \frac{F}{i\omega d} \tag{2.8}$$

Since $i\omega x = \frac{dx(t)}{dt}$ and $Z = \frac{F}{v}$ the impedance is given by 2.9, where v denotes the particular velocity.

$$d = \frac{F}{i\omega x_p} = \frac{F}{v} = Z \tag{2.9}$$

This leads to the important theory that, for frequencies equal to the eigenfrequencies of a damped oscillator, the damping of the system corresponds to the impedance.

2.4 Helmholtz resonance

One efficient way to absorb acoustic energy is by using a bottle or a jar. The phenomenon is called the Helmoltz resonance. The device consists of a cavity connected to the atmosphere via a narrow duct as illustrated in Figure 2.2. Physically, this resonator resembles a mass and spring system. The fluid in the neck of the resonator corresponds to the mass of the oscillator and the cavity corresponds to the spring[3].

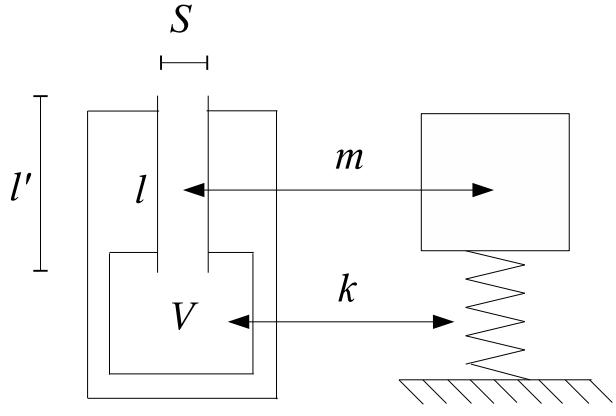

Figure 2.2: The Helmholtz's resonator corresponds to a mass and spring system. The duct of the resonator represents the mass, and the cavity represents the spring of the system.

Due to the cyclic pressure fluctuations in the cavity the fluid (or the mass) oscillates back and forth in the neck. This oscillation results in low tones at the natural (or resonance) frequencies. The natural frequencies can be calculated with Equation 2.10 [5], where S denotes the area of the opening of the bottleneck and V is the volume of the cavity. l' is given by Equation 2.11 and denotes the length of the neck, corrected because of the moving air outside the edge[5].

$$f_0 = \frac{c}{2\pi}\sqrt{\frac{S}{l' \cdot V}} \tag{2.10}$$

$$l' = l + 1.7 \cdot \sqrt{\frac{S}{\pi}} \tag{2.11}$$

In order to generate this absorption of acoustic energy the cavity walls have to be rigid and the cross section of the neck has to be much smaller than the cross-section of the cavity[3]. The analogy between the Helmholtz resonance and the resonance of the mass and spring system is illustrated in table 2.3.

mass	$\sqrt{\frac{l'}{S}}$	m
stiffness	$\frac{1}{V}$	k
Resonans frequency	$\frac{c}{2\pi}\sqrt{\frac{S}{l'V}}$	$\frac{1}{2\pi}\sqrt{\frac{k}{m}}$

Figure 2.3: The analogy between the mass and spring system and the Helmholtz's resonator. The smaller cross section and longer pipe, the more damping you get.

2.5 Internal Energy Loss

2.5.1 Introduction

In chapter 2.1 the reader was introduced to the wave equation. This equation applies for waves with adiabatic propagation and no internal losses. For wave propagation in small ducts, and sharp corners, internal energy losses due to viscosity and thermal conduction have to be accounted for. Thus, the wave equation has to be modified in order to include these losses.

2.5.2 Boundary layers

Near the boundaries, visco-thermal effects on the sound wave is important in regions called viscous boundary layers and thermal boundary layers. In figure 2.4 viscous boundary layers are illustrated. The alternating difference in pressure causes a motion of the air molecules between the walls. Half way between the walls the maximum amplitude of motion will occur, while the molecules in contact with the walls remain at rest. This velocity difference between the molecule layers gives rise to frictional losses near the the walls as marked by (δ_{visc}) in the figure. The thickness of the viscous boundary layer, δ_{visc} is given by Equation 2.12[6].

$$\delta_{visc} = \sqrt{\frac{2\mu}{\omega\rho_o}} \tag{2.12}$$

Here μ and ρ_o denote the shear viscosity and the density respectively. The thermal boundary layer is the region where the flow changes character from adiabatic in the mainstream to isothermal near the surface. The thickness of the thermal boundary layer δ_{therm}, is given by Equation 2.13[6].

$$\delta_{therm} = \frac{\delta_{visc}}{\sqrt{Pr}} \tag{2.13}$$

Here Pr denotes the Prandtl's number. A frequency of 1 kHz for air yield $\delta_{visc} =$ 0.06 mm and $\delta_{therm} = 0.076$ mm. Since the two boundary layers obviously are

very thin, the energy dissipation within the layers can be considered to appear *at* the boundaries. At least for large scale problems. For finite dimensions the boundary layers will represent a much greater part of the cavity. A natural consequence from this is that the smaller the dimensions are, the more energy losses you get. Another thing is that the most energy dissipating point doesn't necessarily have to be the one closest to the surface. Obviously it is hard to determine the variation of the energy losses for small scale problems. For this reason it is necessary to use a finite element approach. The Finite Element Method will be described in section 2.7.

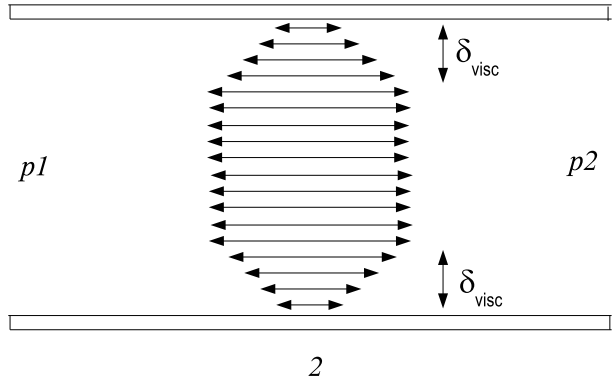

Figure 2.4: The Viscous boundary layers. The thickness of δ_{visc} depends on the distance between the walls, and the viscosity of the fluid.

2.6 The wave equation modified for visco-thermal effects

The mathematical model presented in this work is based on the Navier-Stokes-continuity- and energy equations[6]. The original set of field equations are reduced to a system with two unknowns: the acoustic part of the pressure, p, and the acoustic part of the temperature, τ. Equations 2.14 and 2.15 will be the starting point for the finite element formulation presented in this work[6].

$$\nabla^2 p = \frac{\gamma}{c_a^2}\left(\omega^2 + l_v' c i\omega\nabla^2\right)(p - \alpha\tau) \tag{2.14}$$

$$l_h c\nabla^2\tau = i\omega(\tau - \frac{\gamma - 1}{\gamma\alpha}p) \tag{2.15}$$

Here $\gamma = \frac{C_p}{C_v}$ denotes the ratio of specific heat at constant pressure to the specific heat at constant temperature. The term α denotes the rate of increase of pressure with temperature at constant volume. The vertical and horizontal molecular mean-free-path l_v' and l_h respectively are described in Equation 2.16 and Equation 4.13.

$$l_v' = \frac{\nu + \frac{4}{3}\mu}{\rho c} \tag{2.16}$$

$$l_h = \frac{K}{\rho C_p c} \tag{2.17}$$

Here K denotes the heat conductivity, ν denotes the bulk viscosity and μ denotes the coefficient of shear viscosity. The bulk viscosity is the change in pressure due to isotropic expansion.

From Equations 2.14 and 2.15, two different modes of wave motion can be derived. The first mode is called the *propagational* mode and corresponds to a wave which propagate with an almost adiabatic velocity. For this mode the fluid equation 2.14 is the dominating one. The second mode, which occur for a state where τ is much greater than p corresponds to the heat conduction described in equation 2.15 and is called the *thermal* mode. Which wave predominates depends on the influences of the energy-loss term in l'_v and l_h. The thermal mode is important only within the thermal boundary layer described in Equation 2.13. The velocity vector $\mathbf{u}$, of the fluid plays an important role in this mathematical model. It can be separated into two parts, the longitudinal part u_l, given by Equation 2.18 and a transverse part u_t, given by Equation 2.19 [6].

$$\bar{u_l} = \frac{\nabla p}{\rho i\omega} - \frac{\gamma l}{\rho c}\left[\nabla p - \nabla T\right] \tag{2.18}$$

$$\bar{u_t} = \frac{\mu}{\rho i\omega} curl(curl\bar{u_t}) \tag{2.19}$$

$$u = u_l + u_t \tag{2.20}$$

The longitudinal velocity is the one related to the acoustic pressure according to Equation 2.20. It is therefor coupled to the propagational mode and will be used to fit its boundary condition. The rotational velocity is unrelated to pressure waves but constitute a shear motion which actually gives rise to a third wave mode called the *shear* mode. Similar to the thermal mode the shear mode is only important within the boundary layers. The propagational and the thermal mode, through the set of equations 2.14, 2.15 and 2.18, should be sufficient in order to analyse the acoustic impedance. The shear mode will be neglected in this work.

Chapter 3

The Finite Element Method

3.1 Introduction

The finite element method is a numerical prediction technique. It is used for solving differential equations that are too complex to be solved analytically. The region considered is divided into smaller parts, *finite elements*. Within each element there is a locally defined shape function to which the field variable distribution is approximated to. This way the problem results in a set of algebraic equations. In this paper, the differential equations for the heat conduction and the acoustic fluid shown in Equation 3.4 and 3.9 respectively will be solved by the finite element method. To do this, the including field variables p and τ first have to be separated in a frequency dependent and a spatial part through the approximations in Equation 3.1[7]:

$$p(\mathbf{x},\omega) = \mathbf{N(x)p}(\omega) \tag{3.1}$$

$$\tau(\mathbf{x},\omega) = \mathbf{N(x)}\boldsymbol{\tau}(\omega) \tag{3.2}$$

Here $\mathbf{N}$ is a row matrix containing the shape functions and $\boldsymbol{\tau}$ and $\mathbf{p}$ contain the frequency dependent temperature and the frequency dependent pressure respectively. The differential equations will be multiplied by a weight function w:

$$w = \mathbf{Nc}$$

Since w and $\mathbf{c}$ are an arbitrary function and an arbitrary matrix, w can be written as:

$$w = \mathbf{N}^T\mathbf{c}^T$$

Finally, the matrix $\mathbf{B}$ is defined as

$$\mathbf{B} = \nabla\mathbf{N}$$

Which yield $\nabla p = \mathbf{Bp}$ and $\nabla\tau = \mathbf{B}\boldsymbol{\tau}$. With these statements the finite element equations for the acoustic fluid and the heat conduction can be derived.

3.2 Acoustic fluid

To make a finite element solution of the propagational wave mode described in Equation 2.14, it is necessary to start with the fundamental wave equation, without visco thermal effects. The wave equation 2.1 is given again by Equation 3.3.

$$\nabla^2 p - \frac{1}{c^2}\frac{\partial^2 p}{\partial t^2} = \omega^2 Q \tag{3.3}$$

This time the fluid source Q, i.e the mass inflow per unit volume, is added to the equation. The same equation is rewritten in Equation 3.4:

$$-\omega^2 p + c^2 \nabla^2 p = c^2 \omega^2 Q_a \tag{3.4}$$

Multiplied with an arbitrary function w, and integrated over the region Ω yields Equation 3.5:

$$-\omega^2 \int_\Omega w p d\Omega - c^2 \int_\Omega w \nabla^2 p d\Omega = c^2 \omega^2 \int_\Omega w Q_a d\Omega \tag{3.5}$$

The second term can be integrated by parts, giving

$$c^2 \int_\Omega w \nabla^2 p d\Omega = c^2 \int_\Gamma w \nabla p n d\Gamma - c^2 \int_\Omega \nabla w \nabla p d\Omega \tag{3.6}$$

Applying the concepts introduced in the previous section the FE-formulation of the acoustic fluid is giving by Equation 3.7 and is formulated in matrixes in Equation 3.8. The index a stands for acoustic fluid.

$$-\omega^2 \int_\Omega \mathbf{N}^T \mathbf{N}_a d\Omega \mathbf{p} + c^2 \int_\Omega \mathbf{B}^T \mathbf{B}_a d\Omega \mathbf{p} = c^2 \omega^2 \int_\Omega \mathbf{N}_a^T \frac{dQ_a}{dn} d\Omega + c^2 \int_\Gamma \mathbf{N}^T \frac{\partial p}{\partial n} d\Gamma \tag{3.7}$$

$$\left(-\omega^2 \mathbf{M} + \mathbf{K}\right) \mathbf{p} = \mathbf{f}_q + \mathbf{f}_l \tag{3.8}$$

Where:

$$\begin{aligned} \mathbf{M}_a &= \int_\Omega \mathbf{N}^T \mathbf{N}_a d\Omega \\ \mathbf{K}_a &= c^2 \int_\Omega \mathbf{B}^T \mathbf{B}_a d\Omega \\ \mathbf{f}_q &= c^2 \omega^2 \int_\Omega \mathbf{N}_a^T \frac{dQ_a}{dn} d\Omega \\ \mathbf{f}_l &= c^2 \int_\Gamma \mathbf{N}_a^T \nabla \mathbf{p} \cdot n d\Gamma \end{aligned}$$

$\mathbf{f}_l$ is the acoustic load acting on the boundary surface Γ. Equation 3.8 now constitute the foundation to the finite element formulation of the propagational wave mode.

3.3 Heat conduction

In a similar manner as for the propagational wave mode, the finite element formulation for the original thermal conduction has to be defined in order to

solve the thermal wave mode. The differential equation for heat conduction is given in Equation3.9[2]:

$$-\nabla^T \mathbf{q} + Q_h = -\rho c i\omega\tau \tag{3.9}$$

Where $\mathbf{q}(\mathbf{x}, t)$ is the heat flux vector, and Q_h is the heat supply. The index h stands for heat conduction. Similar to the case of the acoustic fluid, Equation 3.9 is multiplied by w and integrated over the region Ω. This yields Equation 3.10[2].

$$-\int_\Omega w\rho c i\omega\boldsymbol{\tau} d\Omega + \int_\Omega w\nabla^T \mathbf{q} d\Omega = \int_\Omega w Q_h d\Omega \tag{3.10}$$

By introducing the fact that the heat flux vector depends on the temperature gradient according to Fourier's law of heat conduction: $\mathbf{q} = -\mathbf{D}\nabla\tau$[2], Equation 3.10 is given by Equation 3.11. The matrix formulation of the heat conduction is given by Equation 3.12.

$$-\int_\Omega \rho c \mathbf{N}^T \mathbf{N}_h i\omega d\Omega\boldsymbol{\tau} + \int_\Omega \mathbf{B}^T \mathbf{D}\mathbf{B}_h d\Omega\boldsymbol{\tau} = -\int_\Gamma \mathbf{N}_h^T q_n d\Gamma + \int_\Omega \mathbf{N}_h^T Q_h d\Omega \tag{3.11}$$

$$\left(-i\omega\mathbf{M}_h + \mathbf{K}_h\right)\boldsymbol{\tau} = \mathbf{f} \tag{3.12}$$

Where:

$$\begin{aligned} \mathbf{M}_h &= \int_\Omega \rho c \mathbf{N}^T \mathbf{N}_h d\Omega \\ \mathbf{K}_h &= \int_\Omega \mathbf{B}^T \mathbf{D}\mathbf{B}_h d\Omega \\ \mathbf{f} &= -\int_\Gamma \mathbf{N}_h^T q_n d\Gamma + \int_\Omega \mathbf{N}_h^T Q_h d\Omega \end{aligned} \tag{3.13}$$

The material parameters ρ and c are defined by the thermal conductivity in the constitutive matrix $\mathbf{D}$.

$$\mathbf{D} = \begin{bmatrix} k_{xx} & 0 & 0 \\ 0 & k_{yy} & 0 \\ 0 & 0 & k_{zz} \end{bmatrix}$$

Here k_{xx}, k_{yy} and k_{zz} denote the thermal conductivity in x-, y- and z direction respective. Air is an isotropic material. This means that the thermal conductivity is the same in all directions.

Chapter 4

FE- modeling

4.1 Geometry

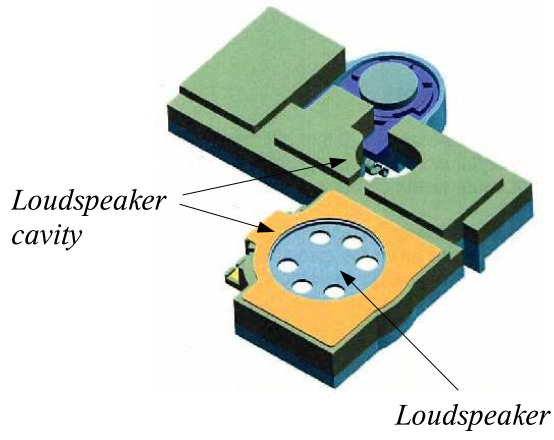

Figure 4.1: The loudspeaker component

The loudspeaker is situated on top of the phone on the backside. Besides generating speech when the phone is turned on to speaker mode it also generates ring melodies and messenger signals. Figure 4.1 shows the loudspeaker component, which consists of a plastic form with a cavity where the loudspeaker is situated. The idea was to make a model similar to this loudspeaker cavity, but without the loudspeaker. Simplified, this empty cavity forms two smaller cavities connected with a narrow duct as shown in Figure 4.2.

Even if the geometry is simplified, it still has to generate eigenfrequencies in the frequency range of interest, namely between 200 and 18000 Hz. Consider the loudspeaker cavity as the spring system in Figure 4.3(a). Connecting the springs parallel, as figured in Figure 4.3(b), the system corresponds to a helmoltz's

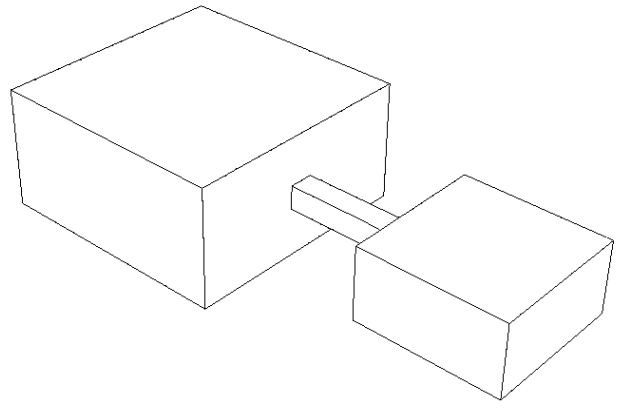

Figure 4.2: The loudspeaker cavity, simplified.

resonator. The effective volume V_{eff}, of the cavity is given by Equation 4.1.

$$V = V_{eff} = \frac{1}{\frac{1}{V_1} + \frac{1}{V_2}} \tag{4.1}$$

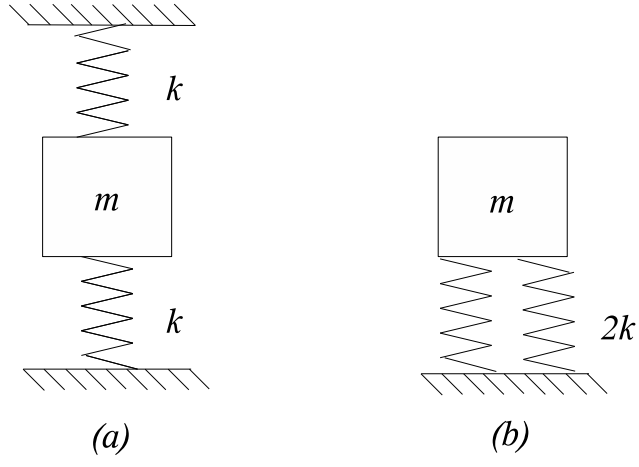

Figure 4.3: The loudspeaker cavity as a mass and spring system(a) and the system parallel coupled(b).

From the statement above and Equation 2.10 and 2.11 from the theory of Helmoholtz's resonator, the model shown in Figure 4.6 should generate a first resonance frequency at 2.4 kHz. The two cavities are deliberately made in different sizes in order to prevent possible effects of symmetry. The model has the dimensions according to table 4.1.

[h] $H1$	5 mm
$A1$	100 mm^2
$H2$	3 mm
$A2$	36 mm^2
S	1 mm^2
V_{eff}	88.8 mm^3

Table 4.1: The Dimensions of the cavity. $H1$ and $H2$ denote the height of the large and the small cavity respectively. $A1$ and $A2$ denote the areas of the two cavities. V_{eff} is the effective volume calculated according to the theory of Helmholtz's resonator and the mass- and spring system in section 2.3 and 2.4.

4.2 Boundary conditions

In order to solve the differential Equations 3.8 and 3.12, relevant boundary conditions have to be specified. The model described above will be given two different boundaries for the two wave modes, see Figure 4.3.3.

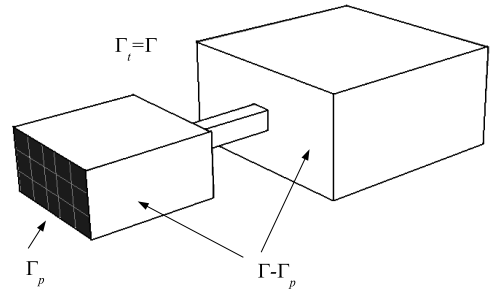

Figure 4.4: The thermal boundary Γ_t, covers the entire surface where $\tau = 0$. On Γ_p and $\Gamma - \Gamma_p$ the velocity is set to 1 and 0 respectively.

For the propagational wave mode the total surface Γ is divided in two. The boundary Γ_p represents the leftmost surface and the boundary $\Gamma - \Gamma_p$ represents the remaining surface. The entire surface Γ is imposed by a time harmonic load with velocity amplitude v, described in Equation 4.2.

$$p = \rho i \omega v \tag{4.2}$$

In order to generate pressure fluctuations in the cavity the velocity amplitude is set to 1 on Γ_p and to 0 on $\Gamma - \Gamma_p$. This means that all the boundaries are infinitely rigid, except for the entire leftmost surface which is vibrating back and forth like a piston. All the nodes on this side have the same displacement. I.e it is considered as an ideal loudspeaker membrane. The boundary for the thermal wave mode Γ_t, is the total surface, i.e $\Gamma_t = \Gamma$. Since the influence of surrounding walls are neglected in this investigation, the acoustic part of the temperature on this boundary is set to 0. The intention of this was to define a perfect heat flow through all the walls. The boundary conditions are summarized in Equation 4.3.

$$\begin{aligned} \tau(\Gamma_t) &= 0 \\ v(\Gamma_p) &= 1 \\ v(\Gamma - \Gamma_p) &= 0 \end{aligned} \tag{4.3}$$

4.3 The Finite element formulation including loss of energy

The set of Equations 2.14, 2.15 and 2.18 forms the starting point of the finite element solution that will include the visco- thermal effects. It will be solved using two different elements, a three dimensional acoustic element for the propagational mode and a three dimensional heat conduction element for the thermal mode.

4.3.1 Propagational wave mode

The propagational wave mode is written again in Equation 4.4. It is rearranged in Equation 4.5, and Equation 4.6 defines again its velocity boundary conditions.

$$\nabla^2 p = \frac{\gamma}{c_a^2}\left(\omega^2 + l_v' ci\omega\nabla^2\right)(p - \alpha\tau) \tag{4.4}$$

$$\nabla^2 p \frac{\gamma\omega^2}{c^2 - \gamma l_v ci\omega} p = \frac{\gamma\omega^2}{c^2 - \gamma l_v ci\omega}\alpha\tau - \frac{\gamma i\omega l_v c\alpha}{c_a^2 - \gamma l_v ci\omega}\nabla^2\tau \tag{4.5}$$

$$\begin{aligned} u_l(\Gamma_p) &= 1 \\ u_l(\Gamma - \Gamma_p) &= 0 \end{aligned} \tag{4.6}$$

Equation 4.5 is first multiplied with an arbitrary weight function w, and integrated over the volume.

$$\int_\Omega w\nabla^2 p d\Omega - \omega'\omega\int_\Omega w p d\Omega = \omega'\omega\alpha\int_\Omega w\tau d\Omega - i\omega' l_v c\alpha\int_\Omega w\nabla^2\tau d\Omega \tag{4.7}$$

Where

$$\omega' = \frac{\gamma\omega}{c^2 - \gamma l_v ci\omega} \tag{4.8}$$

The statements from the two previous sections and the divergence theorem yield the FE formulation below. Equation 4.9 shows the matrix-formulation where the indexes p and t stand for the propagational mode and the thermal mode

respective.

$$\int_\Omega \mathbf{B}^T\mathbf{B}_p d\Omega\mathbf{p} + \omega'\omega \int_\Omega \mathbf{N}^T\mathbf{N}_p d\Omega\mathbf{p} - \\ - \int_{\Gamma_p} \mathbf{N}^T\nabla\mathbf{p} n d\Gamma_p = \\ = \omega'\omega\alpha \int_\Omega \mathbf{N}^T\mathbf{N}_t d\Omega\boldsymbol{\tau} + \\ + i\omega' l_v c\alpha \left[\int_{\Gamma_T} \mathbf{N}^T\nabla\tau n d\Gamma_T - \int_\Omega \mathbf{B}^T\mathbf{B}_t d\Omega\boldsymbol{\tau}\right]$$

$$(\mathbf{K}_p + \omega'\omega\mathbf{M}_p)\,\mathbf{p} = \mathbf{Q} + \mathbf{f}_l \tag{4.9}$$

$$\begin{aligned} \mathbf{K}_p &= \int_\Omega \mathbf{B}^T\mathbf{B}_a d\Omega \\ \mathbf{M}_p &= \int_\Omega \mathbf{N}^T\mathbf{N}_a d\Omega \\ \mathbf{f}_l &= \int_{\Gamma_p} \mathbf{N}^T\nabla\mathbf{p} n d\Gamma_p \end{aligned} \tag{4.10}$$

Where $\mathbf{Q}$ still is the mass inflow per unit volume and time, this time according to Equation 4.11:

$$\mathbf{Q} = -i\omega' l_v c\alpha\mathbf{K}_t - \omega'\omega\alpha\mathbf{C}\boldsymbol{\tau} + i\omega' l_v c\alpha \int_{\Gamma_t} \mathbf{N}^T\nabla\tau n d\Gamma_t \tag{4.11}$$

The acoustic load $\mathbf{f}_l$ is acting on the total boundary surface Γ. From Equation 3.6 yield ∇p:

$$\nabla p = \frac{i\omega\rho u_l - \frac{\gamma l_v}{c} i\omega\alpha\nabla\tau}{1 - \frac{\gamma l_v}{c} i\omega} \tag{4.12}$$

Applying the boundary conditions, Equation 4.12 gives $\nabla p = \frac{i\omega\rho - \frac{\gamma l_v}{c} i\omega\alpha\nabla\tau}{1 - \frac{\gamma l_v}{c} i\omega}$ for $u_l = 1$ on the vibrating side Γ_p. On remaining surfaces $\Gamma_t - \Gamma_p$, the boundary condition $u_l = 0$ yields $\nabla p = \frac{-\frac{\gamma l_v}{c} i\omega\alpha\nabla\tau}{1 - \frac{\gamma l_v}{c} i\omega}$. From the derivation above it turns out that the mass matrix $\mathbf{M}_p$ is identical to original mass matrix $\mathbf{M}_a$ for the case without visco-thermal effects, while the stiffness matrix $\mathbf{K}_p$ has to be modified for the lack of the velocity term c^2 to correspond to $\mathbf{K}_a$. This is done by changing the input value $c = 340$ to $c = 1$ in the implementation.

4.3.2 Thermal wave mode

The heat conduction from Equation 4.5 is defined by the thermal mode, given again by Equation 4.13.

$$l_h c\nabla^2\tau = i\omega(\tau - \frac{\gamma - 1}{\gamma\alpha} p) \tag{4.13}$$

Equation 4.13, is treated in the same way as for the propagational mode:

$$\int_\Omega \mathbf{B}^T\mathbf{B}_t d\Omega\boldsymbol{\tau}+\frac{i\omega}{l_h c}\int_\Omega \mathbf{N}^T\mathbf{N}_t d\Omega\boldsymbol{\tau} = \int_{\Gamma_T}\mathbf{N}^T\frac{d\tau}{dn}d\Gamma_T+\left(\frac{\gamma-1}{\gamma\alpha}\frac{i\omega}{l_h c}\right)\int_\Omega \mathbf{N}^T\mathbf{N}_p d\Omega\mathbf{p} \tag{4.14}$$

With the matrix formulation 2.1:

$$(\mathbf{K}_t + k\mathbf{M}_t)\tau = \frac{\gamma-1}{\gamma\alpha}\frac{i\omega}{l_h c}\mathbf{M}_p\mathbf{p} + \int_{\Gamma_t}\mathbf{N}^T\frac{d\tau}{dn}d\Gamma_t \tag{4.15}$$

$$\begin{aligned}\mathbf{K}_t &= \int_\Omega \mathbf{B}^T\mathbf{B}_t d\Omega \\ \mathbf{M}_t &= \int_\Omega \mathbf{N}^T\mathbf{N}_t d\Omega\end{aligned} \tag{4.16}$$

$\int_{\Gamma_t}\mathbf{N}^T\frac{d\tau}{dn}d\Gamma_t$ is the temperature gradient on the boundary Γ_t. Here $k = \frac{i\omega}{l_h c}$ is the thermal conductivity. Comparing to the original heat conduction matrix K_h, k has to be set to one in the constitutive matrix $\mathbf{D}$.

4.3.3 Summary of the calculations

An iteration between Equations 4.9 and 4.15 should yield a converged value of the acoustic pressure, included the visco-thermal effects. In order to make the calculations more perspicuous a summary of the calculation procedure is presented in Figure 4.3.3. The values of the parameters introduced in this model is given in table 4.2.

μ	$184.6 \cdot 10^{-7}$	(Ns/m^2)
ν	$110 \cdot 10^{-7}$	(Ns/m^2)
ρ	1.1614	(kg/m^3)
c	340	(m/s)
α	$3.66 \cdot 10^3$	
γ	260	

Table 4.2: The values of the parameters used in this model.

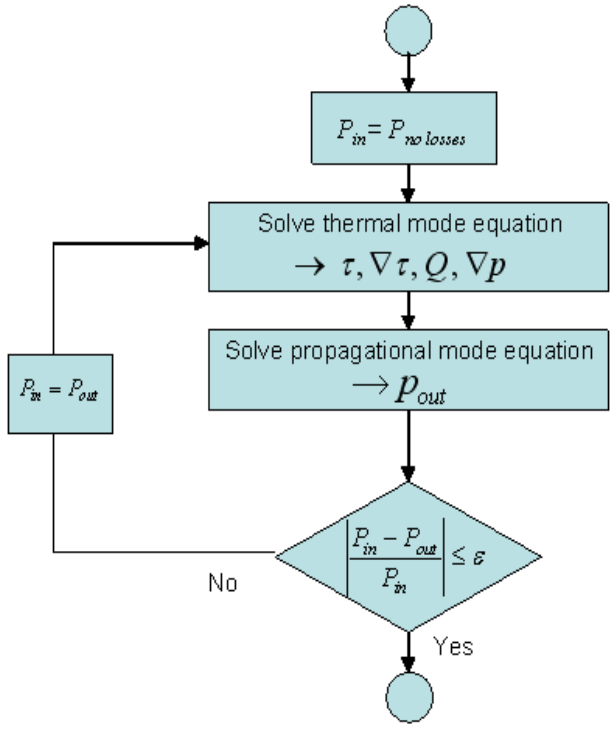

Figure 4.5: The calculation flow chard. For each frequency in interest the procedure starts with p_{in}, i.e the pressure without internal energy losses. The first step is to solve the thermal wave mode, Equation 4.15, which yields τ and $\nabla\tau$. With these temperature parameters Q and ∇p can be solved, by Equation 4.11 and 4.12 respectively. The second step is to solve the propagational wave mode, Equation 4.9 ending up in a "new" acoustic pressure p_{out}. The procedure from the first step to the second will be iterated until the acoustic pressure has converged according to the criteria: $|\frac{p_{in}-p_{out}}{p_{in}}| = epsilon = 0.1$.

4.4 Simulations in ABAQUS

4.4.1 Introduction

A useful tool to solve finite element problems is the computer simulation program ABAQUS.CAE. One of its limitations is off course that it does not totally include the problem introduced in this work. This section will give a brief presentation of the simulation procedure in ABAQUS.CAE. Since the drawing and the mesh application of the model are very straight forward, these will not be payed any further attention. The mesh is illustrated in Figure 4.6. For beginners the basic tutorial and the user's manual "Getting started" are highly recommended.

4.4.2 Internal energy losses in ABAQUS

In ABAQUS the internal energy losses are applied by defining a flow resistance called *volumetric drag*, γ [1]. Equation 4.17 shows the analogy between the flow resistance and the viscous fluid losses.

$$\gamma = \frac{\omega^2 \rho}{B}(\nu + \frac{4}{3}\mu) \tag{4.17}$$

Here B denotes the bulk module ($B = \rho \cdot c^2$) and ν again, the bulk viscosity. In the ABAQUS interface, this volumetric drag is added as a damping constant to the undamped case. It only influences the frequency response at the resonance frequency for which it will decrease the amplitude. The Equation 4.17 is found in the ABAQUS user's manual, where it is only recommended for porous absorbents, for example mineral wool. In the telephone production it can bee used, however, as a "steering wheel". This means that the volumetric drag is tuned to get a certain damping, instead of refining the frequency response afterwards. For the loudspeaker's properties Equation 4.17 yields a volumetric drag of $4 \cdot 10^-6$. This is too small to affect the frequency response. Instead the volumetric drag for this model is set to 200.

4.4.3 Material and boundary conditions

In the property module the material behaviors *acoustic medium* and *density* were chosen. For the acoustic medium The bulk modulus $B = \rho c^2$ and the volumetric drag were defined. The material properties were set according to table 4.2. Since the surfaces for an acoustic medium in ABAQUS are rigid by default, no velocity boundary conditions needed to be specified. Note that there is no possibility to apply any heat conduction for an acoustic medium. The load applied at the leftmost surface was created in the load module. It was defined as an *inward volume acceleration* with magnitude $1 + 0i$ and amplitude $2\pi f$.

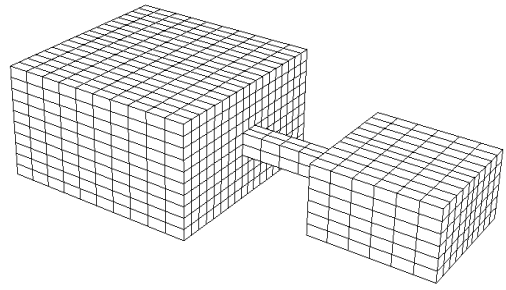

Figure 4.6: The loudspeaker cavity with the mesh, drawn in ABAQUS.

Chapter 5

Simulation Results

The first step was to investigate the impedance without visco- thermal effects. This was done by implementing Equation 3.9 using a three dimensional acoustic element in Calfem. The Impedance is shown in Figure 2.10 and is called the *base case*. The peaks are infinite, but is not noticeable in this figure because of the resolution. The peak of the impedance at a frequency of 2.4 kHz, which was outlined in section 6 confirms the resonance phenomena of the cavity geometry. Figure 2.11 shows the comparison between the base case from Calfem, the corresponding base case made in ABAQUS and the frequency response from ABAQUS included a volumetric drag of 200. Here the impedance is calculated for a frequency range including only the first resonance frequency of the model in order to avoid pressure differences within the elements. As can be seen, the volumetric drag decreases the amplitudes only at the resonance frequencies. According to Figure 2.11, the calculations in Calfem without visco- thermal effects, are comparable to the calculations in ABAQUS without the damping constant volumetric drag. [6]. The last figure shows the base case from ABAQUS and the frequency response with the energy losses included according to the calculations. The response seems to be totally damped by the energy losses. Apparently there is something wrong with the algorithm.

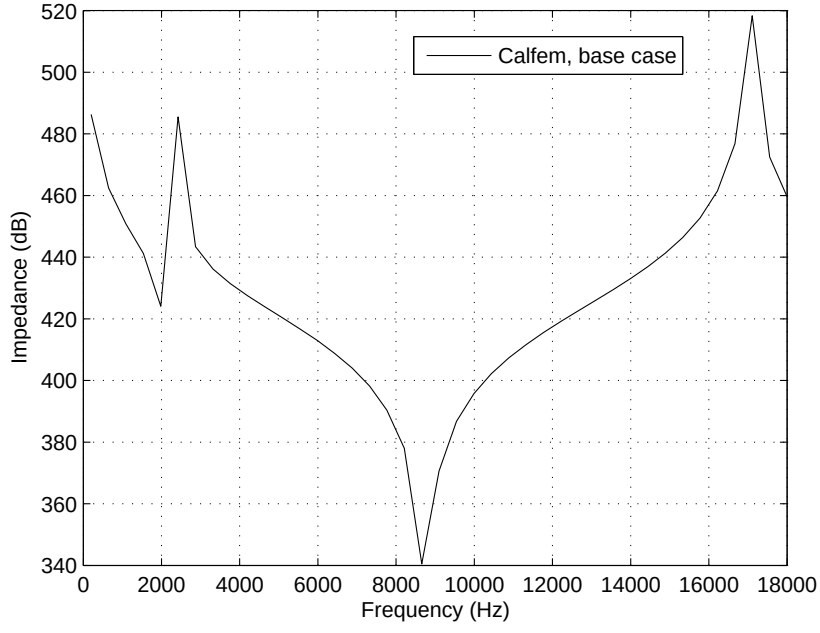

Figure 5.1: The acoustic impedance without visco-thermal effects as a function of frequency. The peak at frequency 2.4 kHz corresponds to the resonance frequency of the loudspeaker cavity.

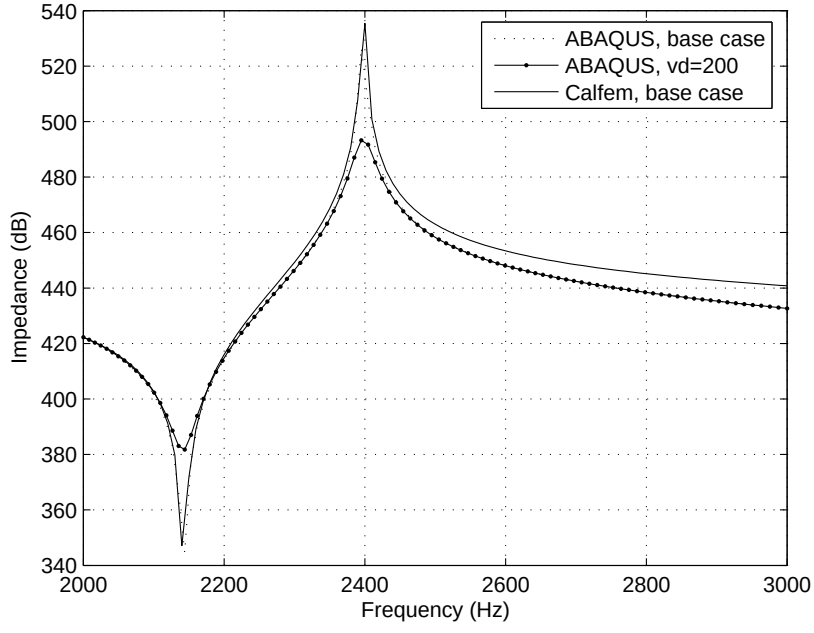

Figure 5.2: The acoustic impedance. The base case from ABAQUS.CAE and Calfem are the same and cover each other. The dotted line shows the impedance included the volumetric drag, $\gamma = 200$.

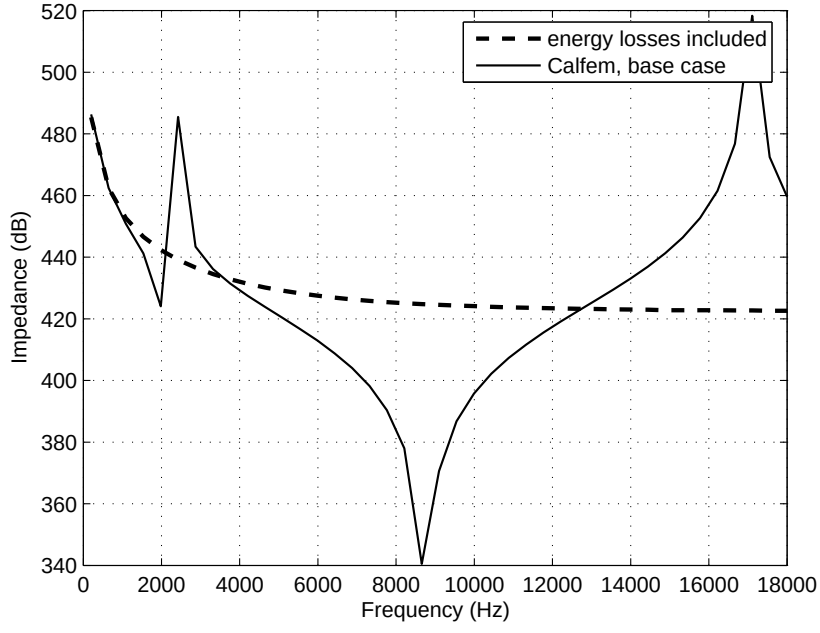

Figure 5.3: The broken line shows the acoustic impedance with internal energy losses included. The solid line is the base case frequency response. From this figure it seems like the energy losses totally damp the system.

Chapter 6

Conclusions

It is clear that the internal energy losses, caused by viscosity and thermal conduction cannot be neglected for all types of geometries. The geometry of the loudspeaker cavity, corresponds to a Helmholtz's resonator. This is demonstrated in Figure 5.1. A consequence of this is that the damping of the system determines the amplitude totally for frequencies equal to the eigenfrequencies. According to the discussion in section 2.3 the damping at the resonance frequencies is equal to the acoustic impedance. For that reason, in order to describe the acoustic impedance in the loudspeaker cavity, it is important to take the energy losses into consideration.

Including the internal energy losses, i.e. the viscosity and thermal conduction in the acoustic impedance is not trivial. In the finite element simulation program ABAQUS.CAE the viscous part of the damping must be set, or calibrated, using the *volumetric drag*. This parameter is described in great detail in the user's manual, but is only recommended for porous materials. It was nevertheless used to analyze its general influence, and to get an idea how the damping would look like. For the loudspeaker's properties Equation 4.17 yields a volumetric drag of $4 \cdot 10^{-6} kg/sm^3$. This value was first implemented in the ABAQUS.CAE model but did not have any influence on the frequency response. Instead the volumetric drag was set to $200 kg/sm^3$. According to Equation 4.17 the value of the volumetric drag is determined by a number of parameters. One of these is the "bulk viscosity", for which it turned out to be difficult to define the relevant type of input. This is probably one reason why there is no general method including all types of materials.

The main reason why ABAQUS is inadequate for this purpose is, however, that it only includes the viscous losses, not the thermal conduction.

When starting this work, the main goal was not to get an accurate and working algorithm but to understand and to explain the phenomena of internal energy losses. The set of equations (Eqs. 7, 8 and 9) has been a common starting point for similar problems, and is not questioned here. The challenge was to attempt to translate it into a finite element model. According to the result in fig 5.3, the model does not seem to work properly. The result should resemble the frequency response from the ABAQUS simulation, where the resonance

frequency amplitude is decreased by the volumetric drag. Instead the algorithm seems to converge to an incorrect value, which results in a totally damped frequency response. This strong damping probably has to do with the thermal boundary conditions. One thing that indicates this is the extreme temperature values (over 1000 degrees). Setting the acoustic part of the temperature to zero on all boundaries doesn't necessarily mean that a perfect heat flow has been established. The definition "acoustic part of the temperature" and how it is meant to be interpreted in the modified wave equation and, above all in its finite element solution is not at all obvious. Another part of the problem is the model. First of all, the pipe is probably to big in relation to the boundary layers presented in 2.5.2. This means that, if the algorithm would have worked as expected, there probably would not be any damping at all. Even if the proportions are good enough to generate some damping, the mesh of the model might be too coarse. To make the energy losses occur properly the thin boundary layer should possibly cover one or more elements in the radial direction. This means that the elements, at least the ones closest to the surface (and only in the pipe, since this is where the losses occur), have to be less than $0.016mm$. That element size would mean 3 million elements, which would exceed the available computational capabilities, in particular with regard to run-time. It would be to much even if the symmetry was used in order to reduce the numbers of elements. Another way to investigate the influence of the boundary layer, without changing the mesh, could be to increase the boundary layer thickness so that it covers the elements closest to the surface. For this purpose the shear viscosity was temporarily set to 0.042, given a boundary layer of $1mm$. This action had no effect on the frequency response. The significations of the bulk viscosity parameter is still unclear, mainly because of lack of information. It seems that there are different types of definitions of the "bulk viscosity", depending on the context. For that reason the application of the bulk viscosity in this model might not be correct.

To analyze why the algorithm is not working requires a more thorough study of the theoretical background, which is beyond the scope of this study. This should be attempted in future work within the topic. One thing could be to further investigate the influence of the boundary layers, and generate a mesh more adopted to the expected boundary layer influence. There are many possibilities to make a better mesh than the one presented in this work. Another thing could be to limit the model to only include the viscous losses, since these probably are the dominating one.

Bibliography

[1] Getting started ABAQUS.CAE Version 6.6.

[2] Per-Erik Austrell and Håkan Larsson. Introduction to finite elements in dynamic analysis. Report, Lund Institute of Technology, 2005.

[3] Robert D. Blevins. *Formulas for natural frequency and mode shape*. Krieger publishing company, Florida, 1995.

[4] R Glav H P Wallin H Bodn, U Carlsson and M Åbom. *Ljud och Vibrationer*. MWL, Stockholm, 2001.

[5] Sven G. Lindblad. *Akustik 4*. Lunds Tekniska Högskola, Lund, 1985.

[6] P. M. Morse and K. U. Ingard. *Theoretical acoustics*. Princeton, New Jersey, 1986.

[7] Niels Ottosen and Hans Petersson. *Introduction to the finite element method*. Prentice Hall, Lund, 1992.